Beams with a slit for mechanical metamaterial design

Dura Fauli, Bernat

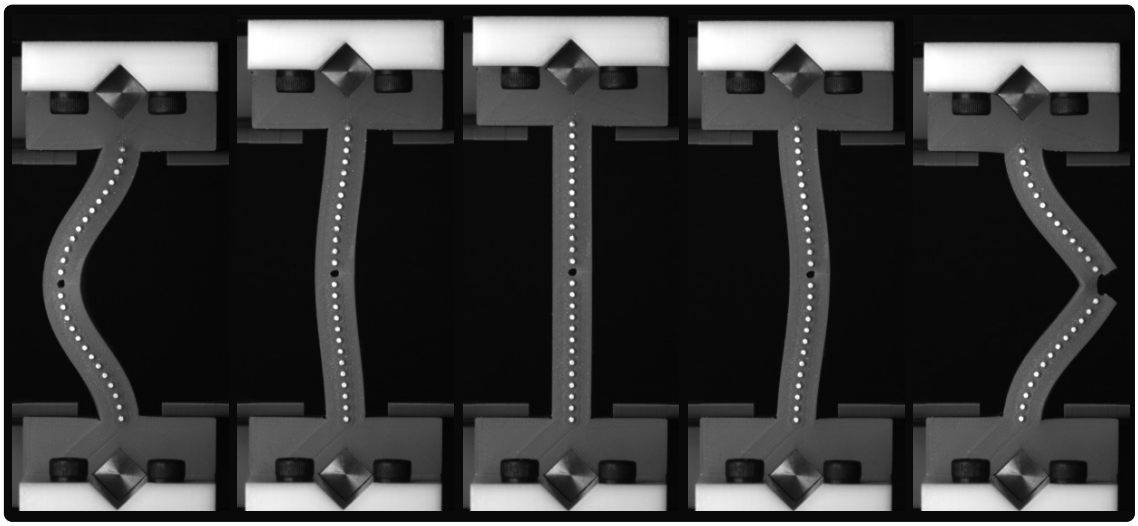

Beams with a slit for mechanical metamaterial design

THESIS

submitted in partial fulfillment of the
requirements for the degree of

MASTER OF SCIENCE
in
PHYSICS

Author :	Bernat Dura
Student ID :	s2312654
Supervisor :	Martin van Hecke
Second corrector :	Daniela Kraft

Leiden, The Netherlands, March 16, 2022

Beams with a slit for mechanical metamaterial design

Bernat Dura

Huygens-Kamerlingh Onnes Laboratory, Leiden University
P.O. Box 9500, 2300 RA Leiden, The Netherlands

March 16, 2022

Abstract

We have investigated the buckling and snapping unstabilities of beams with a slit, both experimentally and numerically, for different geometries. We find that beams with a slit display non-linear symmetry breaking. Specifically they display asymmetric buckled states after symmetrically buckling, a property that can be used in metamaterial design to propagate and amplify symmetry breaking perturbations. We find hysteresis between the "closed" and "open" post-buckling states of the beam and that the transitions between these are snappy. This hysteresis implies that, under compression, these beams are tristable. Exploring two of the states connected by a hysterectic transition, we can regard them as hysterons under a compression field. We find that we can tune the degree of asymmetry as well as the regime where there is hysteresis by modifying the geometrical parameters of the beam. Both the non-linear symmetry breaking and its characteristic as hysterons make beams with a slit useful tools to achieve functionality in metamaterial design.

Contents

Version of March 16, 2022– Created March 16, 2022 - 12:40

Chapter 1

Introduction

Mechanical metamaterials are materials that exhibit exotic properties that arise from their structure rather than their composition. Examples of such materials are metamaterials with a negative Poisson ratio (auxetic) [1] or pentamode materials, tri-dimensional structures that behave similar to a fluid [2]. These exotic properties are often achieved with the careful arrangement of slender elements, such as rods or beams.

More recently metamaterials that focus on having special properties related to information, such as being able to store memory or being able to count have been developed [3], in contrast to the traditional approach of finding exotic mechanical properties in the materials.

One of these materials, a counting metamaterial, serves us as the starting point of this thesis [4]. This structure is an array of beams carefully arranged, that uses different beams, including beams with a slit, to achieve its functionality. In this counter we see that a beam with a slit can undergo spontaneous symmetry breaking and buckle like an ordinary beam, while only becoming asymmetric somewhere in the post buckling regime. This property is used in the structure to change the orientation of a neighbouring beam in one direction but not in the other, which gives the structure the ability to count successive compression cycles.

The property to be symmetric in the linear regime and then become asymmetric in the non-linear regime makes beams with a slit an interesting structure to design metamaterials, and in this work we will investigate why it has this property and how we can tune such beams in order to use them to design metamaterials.

1.1 Types of beams

Bifurcation diagrams are often used to represent the stable states of a beam. In this work we will make use of bifurcation diagrams displaying the mid beam deflection of the stable states as a function of the applied strain.

When compressing an ordinary beam, the mid beam deflection prior to the buckling strain ϵ_b, remains unaltered and zero, as shown in the typical bifurcation diagram for an ordinary beam shown in figure 1.1 a). At the buckling strain the stable line splits into two sta-

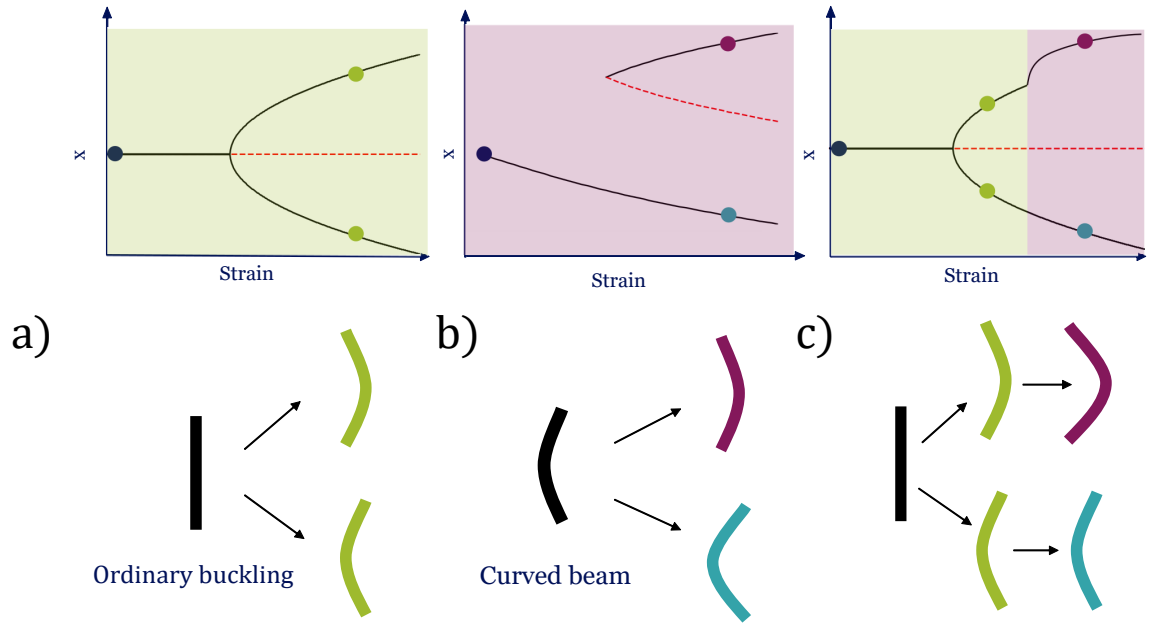

Figure 1.1: *Sketch of the bifurcation diagrams and stable states of an ordinary beam a), and a pre-curved beam b). c) Shows an example of a bifurcation diagram symmetric in the pre-buckling and initial post-buckling regime but asymmetric in the later post-buckling regime corresponding to a desired new beam.*

ble states and one unstable state (red dotted line), representing the beam still being straight. Both stable branches grow monotonically with the square root of the strain and are related by reflection symmetry.

Alternatively, we can use pre-curved beams to obtain a beam with a non-symmetric bifurcation diagram (figure 1.1 b). This might be desired during design to guarantee that the beam will bend in one direction when compressed. The bifurcation diagrams of pre-curved beams have a stable branch that exists continuously for any range of strains, corresponding to the beam bending in its natural pre-curved direction. At a certain strain ϵ_a, another stable branch, together with an unstable branch, appear in the opposite direction of the natural pre-curve. The two stable branches are not related by reflection symmetry.

One of the goals of this work is to achieve a structure with a bifurcation diagram that is symmetric both in the pre and initial post buckling regime, but that becomes asymmetric in the post buckling regime at a given strain, $\epsilon_{pb} > \epsilon_b$ (figure 1.1 c). One could use such a structure to allow the system to decide the buckling direction using small symmetry breaking perturbations, such as a small push on the beam, and having a noticeable different response depending on the choice of direction in the post buckling regime. We will see that a beam with a slit has a diagram with these characteristics.

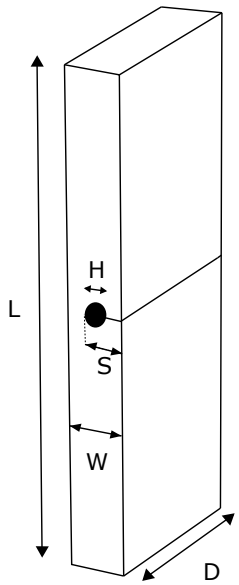

Figure 1.2: *Geometry of a beam with a slit. The beam has vertical length L, width W, and depth D. with$W << L, D$. The slit is located at the right of the beam at a height $L/2$ and has a depth $S < W$. It is terminated with a hole of diameter $H < S$ which center is at a height $L/2$ and at a depth $S - H/2$.*

1.2 Beam with a slit

We define here a beam with a slit as a rectangular beam of height L, depth D and width $W << L, D$ that has a partial cut of its mid beam cross section halfway its length L, along D and of depth $S < W$. The cut creates a slit in the beam that we terminate with a cylindrical hole of diameter $H < S$ to prevent tearing (figure 1.2). The centre of the hole is at a depth $S - H/2$, leaving the total slit size S unmodified. We discuss the effect of the specific values of this parameters in section 4.1.

For the rest of the thesis, we will describe the beam as if it were in the orientation displayed in figure 1.2, where the slit is on the right side of the beam.

1.3 Stable states

We conduct an early exploration of the stable configurations of beams with a slit by performing uniaxial compression experiments under clamped-clamped boundary conditions. This short exploration of the beam's response to compression allows us to distinguish four distinct stable states, depicted in figure 1.3.

The first stable state we can distinguish is the trivial, non-buckled state where the beam is completely straight.

For larger strains, the beam buckles and it can spontaneously do so in both directions, left and right. When the beam buckles left, the beam adopts what we have named the left buckled state, and when it buckles right the beam goes into the closed state. Both states reassemble buckling of an ordinary beam and we will see in section 3.2 that they are symmetric in a certain range of strains.

Version of March 16, 2022– Created March 16, 2022 - 12:40

When the beam buckles right and it's in the closed state, further compression makes it snap and transition into the open state, shown in figure 1.3. This state is clearly distinct from the closed state in its shape, as it has the slit open and its asymmetric with the left buckled state at the same strain.

1.4 Transitions between states

This early exploration allows us to right away catalogue the transitions between states in two groups, those that are smooth and those that are sharp and snappy. The buckling transitions, between the non-buckled and the left buckled or open state, are smooth both during compression and decompression. On the other hand, transitions between the closed and open state are snappy. The beam snaps both when compressing and decompressing. The first snap is the opening transition, going from the closed to the open state and the second snap is the closing transition, going from the open to the closed state.

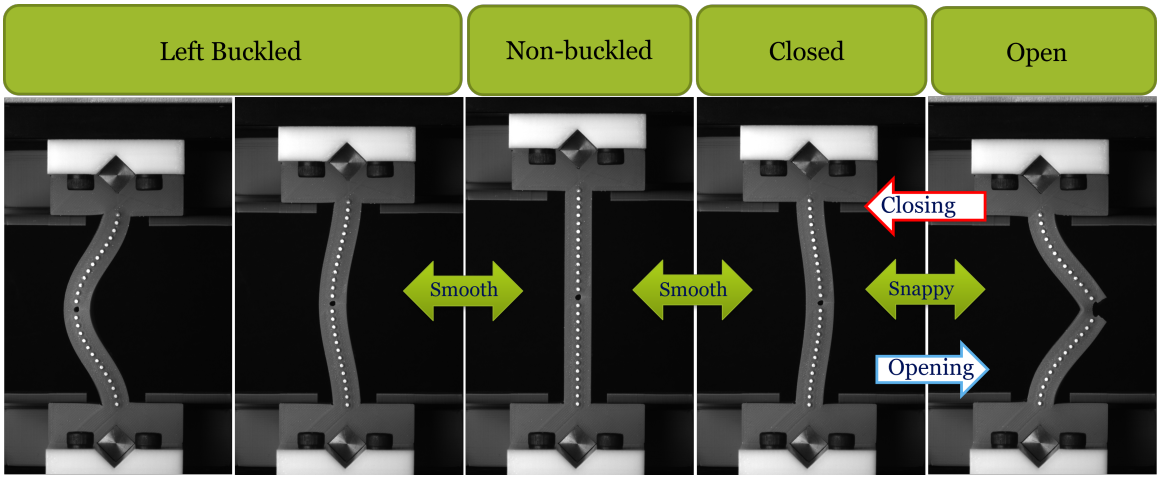

Figure 1.3: *The four distinct states of a beam with a slit: left buckled, non-buckled, closed and open.*

1.5 Bifurcation diagram of a beam with a slit

In order to recover the bifurcation diagram of a beam with a slit, we perform compression experiments on the beams while tracking its mid beam position and the strain applied. In figure 1.4 a), we present the bifurcation diagram of a beam with a slit.

When the beam is under small strains, the mid beam deflection of the beam is null (figure 1.4 a). This is the pre-buckled regime. The beam is in this state for the range of strains comprised between $\epsilon = 0$ and the buckling threshold ϵ_b. Once this threshold is reached, under further compression the beam buckles and the mid beam deflection is no longer zero. We have not explored what happens to the beam when pulling, that is $\epsilon < 0$, and thus we

can't assure that in that regime the beam has a null mid beam deflection.

Once the beam buckles, for $\epsilon > \epsilon_b$, two distinct branches exist, the left branch (blue) and the right branch (orange) (figure 1.4 a). In the bifurcation diagrams negative values of x are associated with the left of the beam and positives values with the right.

1.6 Left branch

When the beam follows the left branch, for $\epsilon > \epsilon_b$, the beam is in the left buckled state. This branch displays a monotonically increase of the mid beam displacement, in absolute values, with the strain. We show that this branch follows a behaviour close to a square root by squaring the x axis of the bifurcation diagram. In this representation the left branch is a straight line, as shown in figure. 1.4 b).

When the beam is decompressed, for $\epsilon >> \epsilon_b$ the mid beam deflection closely matches its compressing counterpart, but near $\epsilon = \epsilon_b$ it decays slower, reaching null mid beam deflection at a strain $\epsilon < \epsilon_b$ (figure 1.4 a). This discrepancy is consequence of the creep of the material and is more pronounced near instabilities, such as the buckling point. Indeed, this discrepancy vanishes for the idealized material of our 2D FEM simulations (figure 1.4 c), pointing that it is a material effect and not a geometrical one.

1.7 Right branch

The phenomenology of the right buckling branch is richer. When crossing the threshold ϵ_b the branch shows a monotonic increase with ϵ, in a similar fashion to the left branch. It is at a larger strain, that the beam undergoes a snapping event that opens the slit. We call such strain the opening strain ϵ_o. This snap marks the transition from the closed to the open state. The snap increases the mid-beam deflection of the right branch drastically and breaks the qualitative symmetry with the left buckling branch (figure 1.4 b). Further compression of the beam, that is in the open state now, shows like its left buckling counterpart, an approximate monotonic square root increase of the mid beam deflection, as shown in figure 1.4 b).

When decompressing the beam, initially the branch follows the same square-root behaviour displayed during compression, and then we observe another remarkable event. The beam, instead of snapping back at ϵ_o, snaps back at a lower strain, the closing strain ϵ_c. One could think at first that the discrepancy between ϵ_o and ϵ_c is due to the creep of the material, similar to the hysteresis displayed by the left branch, but simulations show that this effect is persistent when there is no creep in the material (figure 1.4 c).

After the closing event, the beam proceeds to smoothly reach null mid beam deflection, following a path symmetric to the left branch. We notice that here we find the same hysteresis effect due to creep that we observed in the left branch (figure 1.4 a, b). The curve re-joining null deflection is different from the curve departing null deflection, after buck-

Version of March 16, 2022– Created March 16, 2022 - 12:40

ling, while they are the same in the FEM diagram (figure 1.4 c).

The difference between ϵ_o and ϵ_c at which the opening and closing transitions take place creates a hysteresis loop that gives rise to a strain regime where we have tristability (figure 1.4) opposed to the usual bistability in ordinary buckling. In this regime the beam can be in either of three states: left buckled (figure 1.3 a), closed (figure 1.3 b) or open (figure 1.3 c). Experimentally we have seen that these three states are stable, and it is possible to swap between them by the simple operation of pushing the beam laterally while the beam is under a strain $\epsilon_c < \epsilon < \epsilon_o$. This tristability is not a consequence of material creep, but rather and intrinsic property of beams with a slit, as we still have this regime in FEM simulations (figure 1.4 c).

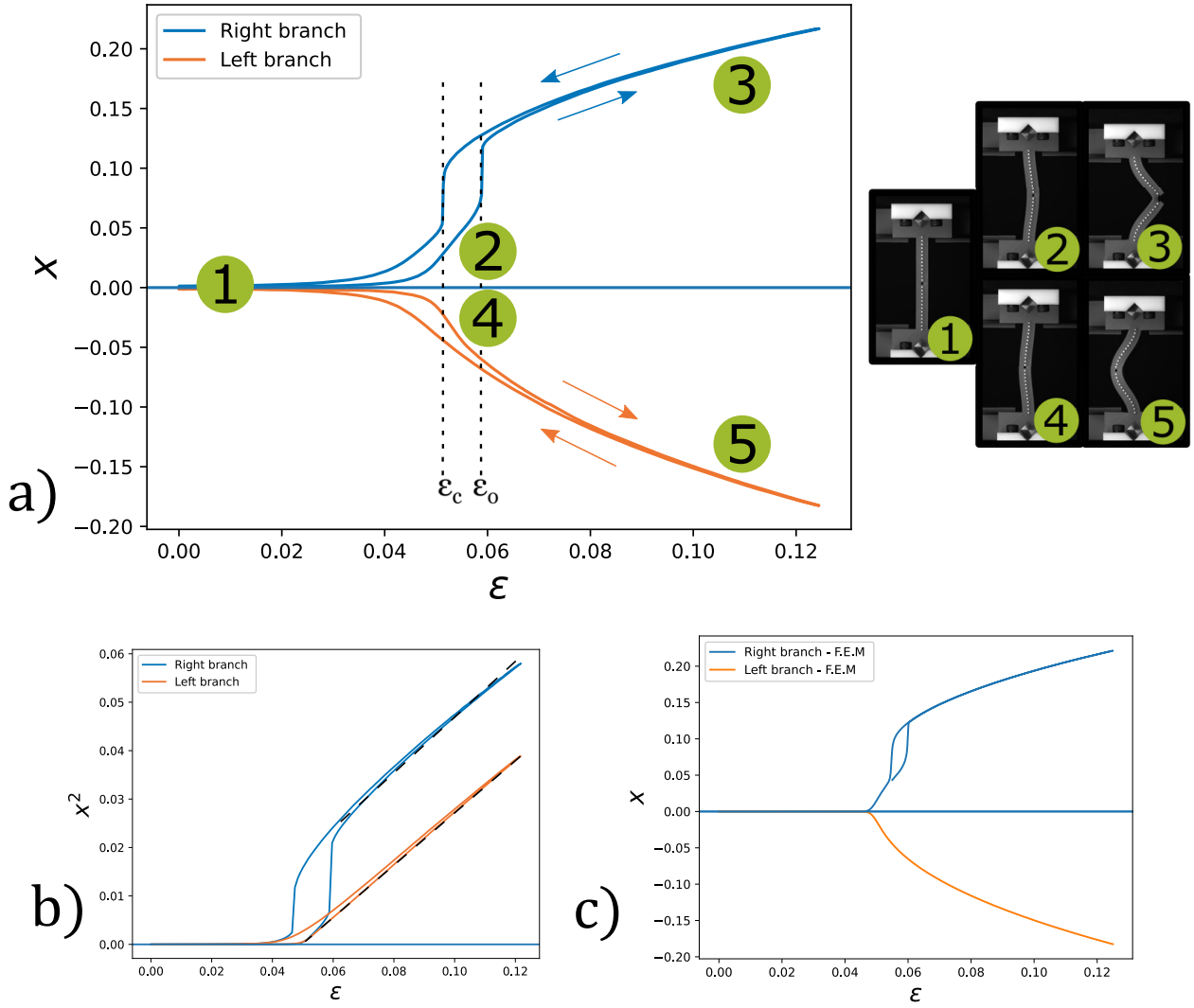

Figure 1.4: *a) Experimentally obtained complete bifurcation diagram for a beam with a slit ($L = 80mm, W = 10mm, D = 25mm, t = 0.125, S = 6mm, H = 2mm$) and localization of the stable states. b) Same diagram as in a) showing the square root behaviour of the branches by squaring x and fitting a simple linear regression (dashed line) to both branches during compression. c) Bifurcation diagram obtained using Abacus/CAE simulations for a 2D beam with slit ($L = 80mm, W = 10mm, t = 0.125, S = 6mm, H = 0.5mm$).*

Chapter 2

Methods

2.1 Manufacturing of the beams

We manufacture the beams by 3D printing (Ultimaker S3, S5) beam molds of PLA with the desired shape and dimension and we cast them with a well characterized silicone (Zhermarck, Elite-Double 22). We have chosen this relatively hard silicone to minimize the effects of gravity on the experiments while still being able to undergo large deformations without breaking or showing significant plasticity. We leave them to cure for at least 6 hours before breaking the mold and then we carefully cut the slit with a scalpel.

2.2 Compression experiments

We carry out experiments in a custom rigid press setup with accurately aligned beam clamps. In our experiments we fix the bottom plate and and apply compression by moving the top plate, which is coupled to a drive system that allows us to have precise dynamical control of its vertical position. We tightly fit the bottom and top supports of our beams to a pair of precisely aligned 3D printed clamps that fix their position and rotation to achieve clamped-clamped boundary conditions. In order to obtain absolute compression values of the beams during the experiments U (figure 2.1), we calibrate the distance between the two plates using a digital height gauge, that allows us to set a point of zero strain. With this reference we are able to obtain the compression applied during the experiments U, as the relative position of the top plate controlled by drive system is known. We normalize U by the rest length of the beam to obtain the strain applied $\epsilon = U/L$ (figure 2.1).

2.3 Image Tracking

We chose to use image tracking to monitor the mechanical response of the beams in our experiments and record a front view of the beam during the experiments using a ccd camera. To facilitate computer analysis of the recorded images we incorporate small dots along the vertical cross section of the beams and paint them white using an edding 8050 tyre marker. We then analyse the images using a custom OpenCV based tracking software to track the

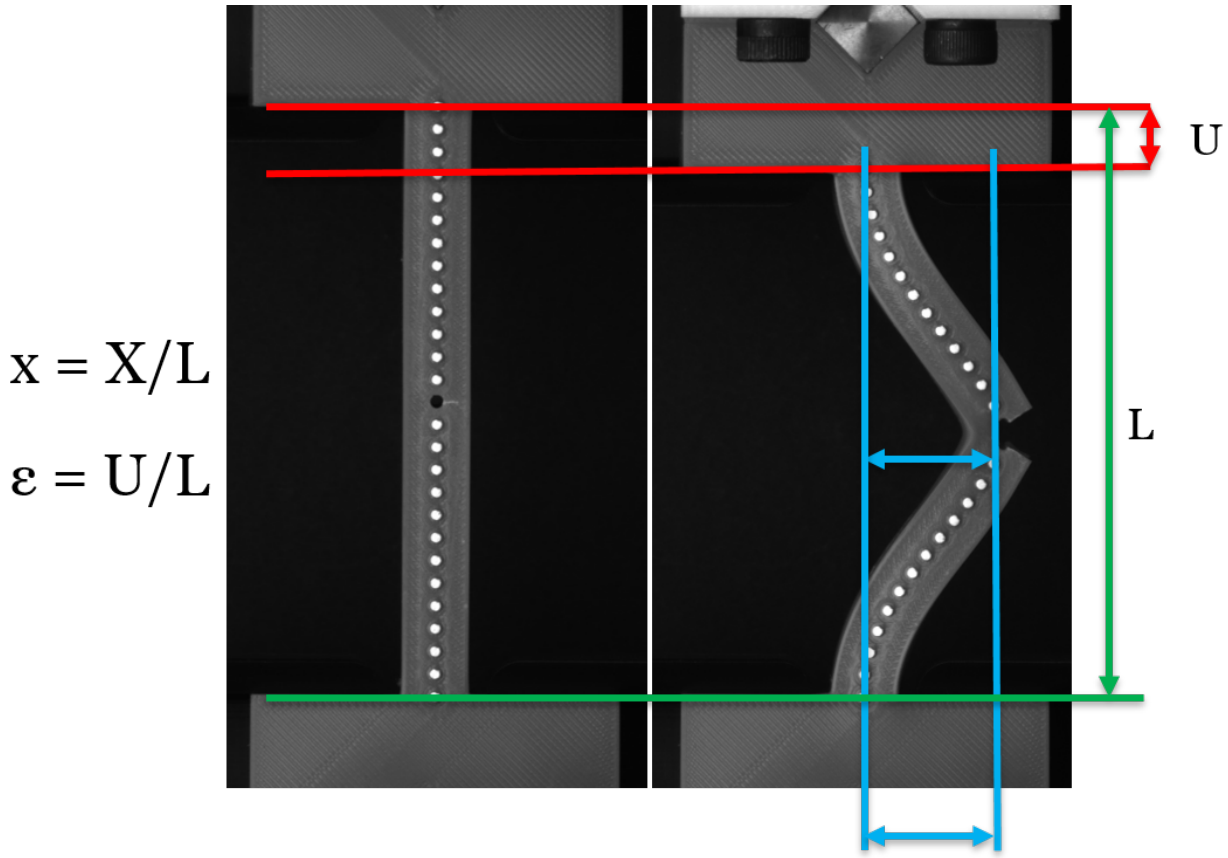

Figure 2.1: *A compression experiment. Left beam is uncompressed. Right beam is in a typical configuration of the right branch in the open state. We record the compression U during the experiments and compute the mid-beam deflection X using image tracking. We then obtain the strain and the normalized mid-beam displacement by dividing these quantities, ϵ and x by the rest length of the beam L.*

white dots, which allows us to obtain the position of the dots at every frame and numerically characterize the deformation of the beam. From this analysis we obtain the mid beam displacement of the beams X, as shown in figure 2.1. We then divide the mid beam displacement by the rest length of the beam to obtain the normalized mid beam displacement x = X/L.

2.4 FEM simulations

2.4.a Simulations details

We recreate in Abaqus/CAE the frontal geometry of our beams with a slit to create a 2D planar and deformable part made of an isotropic Neo-Hookean material with instantaneous moduli time scale.

We choose to map Abaqus/CAE unit of distance to millimetres, the unit of mass to $10^{-9}kg$ and the time unit to miliseconds. Using this references we can give dimensions

Version of March 16, 2022– Created March 16, 2022 - 12:40

to the rest of material parameters and define them to closely reproduce the mechanical response of our experimental beams. Table 2.1 shows the parameters used in the simulations.

For the contact between the top and bottom parts of the slit we define an interaction surface to surface, using the kinematic contact method with finite sliding choosing as surfaces only the top and bottom parts of the slit. We set the friction formulation of the tangential behaviour to rough.

To avoid intersection between surfaces, we need to make the distance between the top and bottom part of the slit nonzero. We make it 0.001, as its the smallest order of magnitude for which errors are not present during the simulations.

Abaqus simulates materials by splitting them up into smaller simpler parts, called finite elements, that together form a mesh. We design the mesh in the mid beam, around the slit in a range of ± 5, to be denser than in the rest of the beam, with the mesh elements being rectangular to avoid rotation of the elements during the simulations, which cause errors.

To simulate the compression experiments we set the boundary conditions to be of the type static, encastre, at the bottom part of the beam and of type displacement/rotation associated to a uniformly increasing and decreasing amplitude in the U2 direction, that compresses the beam in the vertical axis. We then use the explicit protocol to simulate the mechanical response of the beams using a step time to 120000, equivalent to two minutes, to be in quasi static conditions. This time also approximates well the duration of the experiments.

2.4.b Buckling protocol

When simulating the buckling of an ordinary beam in abaqus, the simulations show the beam to be straight for longer that what we see in the experiments, before finally buckling. This is due to the perfect symmetry of the mesh, that together with complete numerical accuracy and dampening, allows the beam to remain longer in the straight unstable equilibrium branch shown in 1.1 a). To correctly access the buckling branch near the buckling point we follow a simulation protocol previously used in other work [5].

The protocol consists in compressing the beam beyond the buckling strain ϵ_b while applying a lateral load at one side of the beam to break the symmetry. We progressively turn off the load following a linear pattern so that we can smoothly reach a buckled state, that remains stable when the load is no longer applied. Next, we decompress the beam until we reach ϵ_b to obtain the buckling branch. To explore the left branch of a beam with slit we apply the same protocol, but due to the opening and closing transitions, to simulate the right branch we need to modify the protocol to correctly asses it.

During compression, we fine tune a lateral load, usually ranging from 15 to 100, so that is large enough to make the beam buckle right but that is small enough to allow the beam to access the buckling branch before the opening transition. This is needed to make the beam buckle in the right direction, as the asymmetry introduced by the finite slit is enough to induce the beam to buckle always left. Then we take advantage of the fact that when de-

Hyperparameters	Value
Density	2000
C10	121590.4394
D1	1.51997E-09
Alpha	0.1
Linear bulk viscosity	0.06
Quadratic bulk viscosity	1.2

Table 2.1: *Material parameters used in Abaqus/CAE simulations.*

compressing, after the closing transition, the beam rejoins the ordinary buckling branch of the beam, to correctly assess the part of the buckling branch that we where not able to correctly asses due to the needed lateral load. We follow this protocols to obtain the bifurcation diagram, disregarding the protocol derived artifacts in the branches as shown in figure 2.2.

To simulate the buckling of the half-beams introduced in section 3.4, we use the same protocol as for ordinary beams.

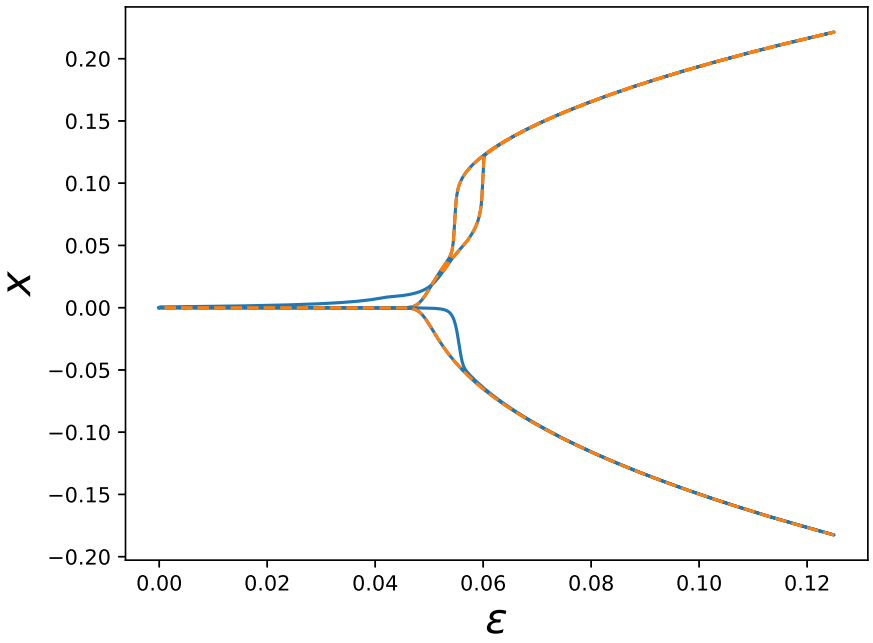

Figure 2.2: *Protocol to obtain the bifurcation diagram from simulations. In blue, the full simulation run. The dashed orange line shows the bifurcation diagram without simulation artifacts.*

2.5 Spring Model for a Beam

We use a simple spring model that is able to reproduce the buckling transitions of both ordinary and pre-curved beams. With only one fit parameter for ordinary buckling, and two fit parameters for pre-curved beams, the model can represent the bifurcation diagram of real beams with good accuracy.

The beam is modeled as two linear springs joined by one torsional spring, as sketched in figure 2.3 a). At rest the system has height L. The energy of the spring system is given by:

$$E = \frac{1}{2}k_l(L_k - A)^2 + \frac{1}{2}k_t(\theta - \theta_k)^2 \tag{2.5.1}$$

Where L_k is is rest length of the linear spring and θ_k the rest angle of the the torsional spring, k_l the spring constant of the linear spring and k_t the spring constant of the torsional spring. For a pre-curved beam we need to introduce another parameter, the natural deflection x_d. We adjust the length of the linear springs to be at rest $L_k = \sqrt{x_d^2 + (L/2)^2}$. This preserves the total height of the beam to be L. We also set the neutral angle of the torsional spring to be $\theta_k = \arctan(x_d/L/2)$.

As all stable solutions have top-down symmetry, the vertical position of the torsional spring is fixed to be (L-U)/2, simplifying in great measure the configuration space that we have to explore to find a stable solution. We find stable solutions of the structure by probing the system's energy varying the horizontal position of the torsional spring. We find that probing the horizontal space left and right a distance L/2, is enough to recover an energy landscape with at least one stable energy minimum, as shown in 2.3 b), c).

Finding the energy minimum for the desired range of strains reproduces the bifurcation diagram of a beam, shown in figure 2.3 d). The position of the enrgy minimums of the system is dependant on the ratio of the stiffness of the linear and torsional springs and not their absolute values. As so, we set the linear spring stiffness to be $k_l = 1$ and the solutions are now only dependent on the parameter $k = \frac{k_l}{k_t}$ and the natural deflection x_d. The ratio k can be considered the equivalent of the parameter t in ordinary beams, as it determines the buckling strain ϵ_b following the same scaling that t has: $\epsilon_b \propto t^2$ and $\epsilon_b \propto k^2$, as seen in figure 2.3 e).

Version of March 16, 2022– Created March 16, 2022 - 12:40

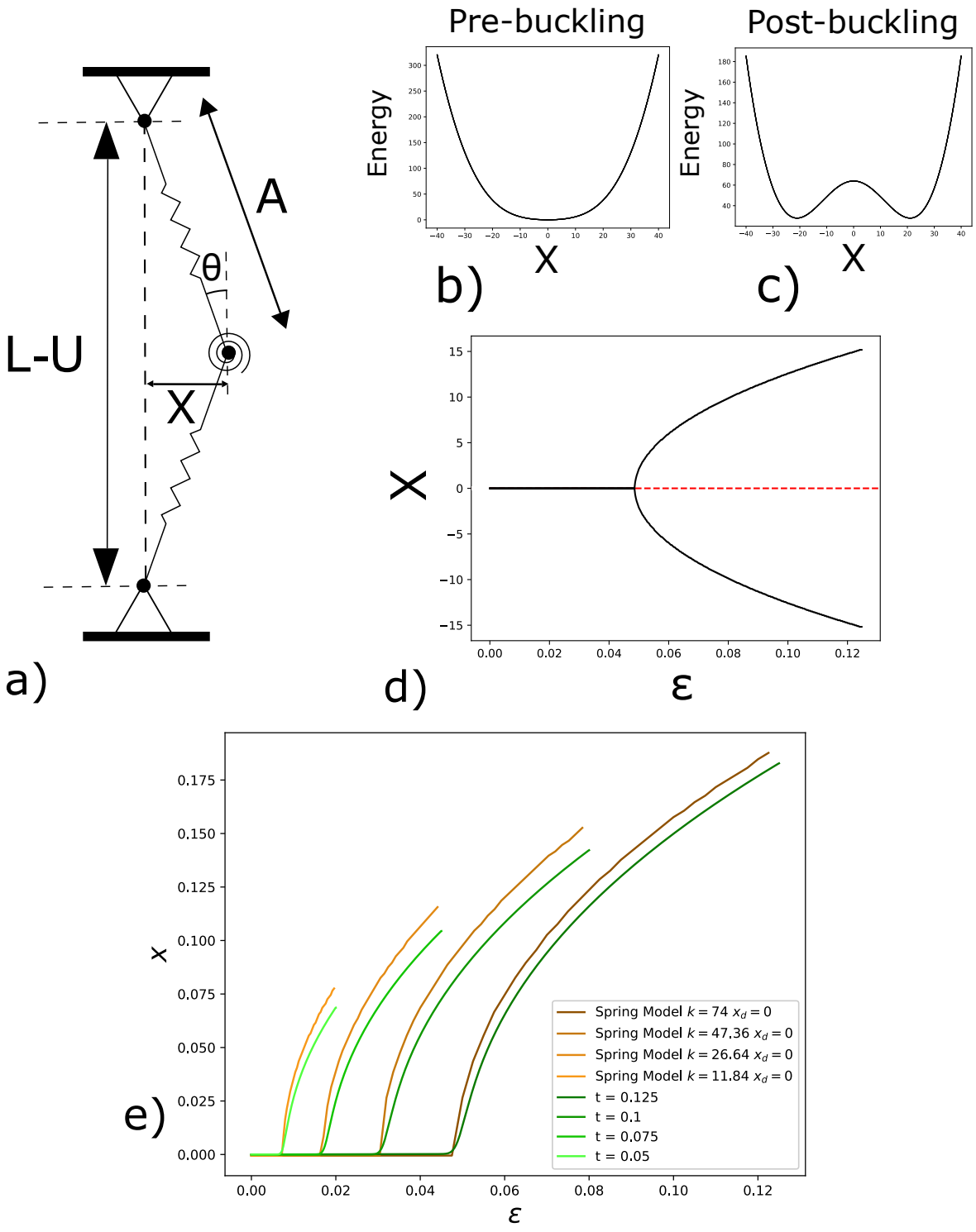

Figure 2.3: *a) Sketch of the spring system used in the buckling of a beam model. b) Energy landscape for a spring system with $x_d = 0$, $L = 80$ and $k = 74$ in the pre-buckling regime. c) Energy landscape for a spring system with $x_d = 0$, $L = 80$ and $k = 74$ in the post-buckling regime. d) Bifurcation diagram constructed by finding the energy minimum on the energy landscapes for different strains. e) Right branch of the bifurcation diagram of ordinary beams with different t compared to the bifurcation diagram of springs systems with different k.*

Chapter 3

States and dynamics of a beam with a slit

To further study and understand the behaviour of beam under compression experiments we now use a finite element method (FEM) software, Abaqus/CAE, to simulate compression experiments on beams with a slit. We have seen that these simulations display the same phenomenology that the one observed in experiments (figure 1.4) and we are confident exploring the beams response using FEM Simulations have a number of advantages over experiments, such as the absence of creep, the fast exploration of different geometries by avoiding the need of having to manufacture samples and that they allow us to study the internal strains and stresses of the beam . We will discuss the specifics of the differences between experimental data and FEM simulations in section 4.2 to assess the validity of the conclusion drawn from our simulation analysis.

3.1 Left buckled state

We have seen that the left buckled state resembles ordinary buckling (figure 1.3). To precisely characterize the left buckled state, and compare it to ordinary buckling, we simulate an ordinary beam, a beam with a hole in the centre, and a beam with a slit with same dimensions L, W and H under clamped-clamped boundary conditions.

We compare the branches corresponding to a regular beam and a beam with a hole, and find that both lie on top of each other precisely, as shown in figure 3.1. The hole ,if small $h < 0.25$, has very little effect on the overall buckling behaviour of a beam. Figure 3.1 also shows that the left buckling branch of a beam with a slit buckles in the same way as a regular beam, and thus we can consider that in this state the slit is has no effect.

3.2 Closed state

We now compare the closed state to the left buckled state, by flipping the left buckled branch. Figure 3.1 shows that both states share the same ϵ_b, and immediately after ϵ_b, the branches are related by symmetry. This is true for the majority of the strain regime comprised between ϵ_b and ϵ_o, but not all.

As the applied strain approaches ϵ_o, we can see that the right branch of the beam with a slit starts to deviate from the regular buckling branch, just before snapping. We define the strain at which this deviation starts as ϵ_{ts}. We can then divide the closed state behaviour in two regimes. In the first regime, $\epsilon_b < \epsilon < \epsilon_{ts}$, the slit has no effect, and the buckling behaviour is identical to a regular beam and symmetric to the left buckled state. In the second regime, $\epsilon_{ts} < \epsilon < \epsilon_o$, this is no longer true, but the beam has not snapped yet and remains in the closed state. We will see in section 3.3 that ϵ_{ts} is the onset of tensile stresses in the mid-beam.

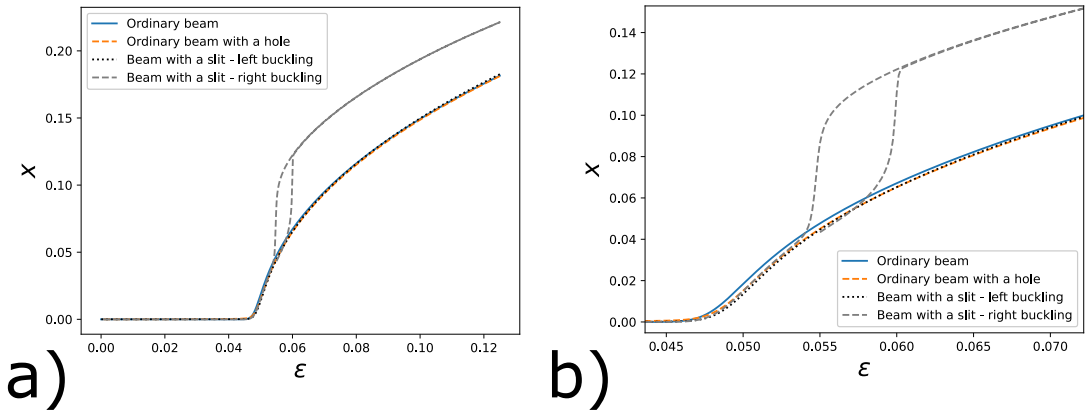

Figure 3.1: *a) Comparison of the bifurcation diagrams obtained by simulating an ordinary beam, an ordinary beam with a hole and both the left and right branches of a beam with a slit. b) Same as a) but zoomed around the buckling point.*

3.3 Opening transition

In this section we will study the opening snapping transition, which drives the beam with a slit from the closed state to the open state.

In order to tackle this task, we have studied the stress profile in the mid beam cross section of a beam. We are only able to recover this magnitudes in Abaqus/CAE simulations, as these allow us to record physical magnitudes that are hard to access experimentally, such as the strain and stresses of the beam at each element.

Obtaining the mid beam profile of a beam with a slit directly is not very helpful. Because the top and bottom parts of the slit cannot be under tensile stresses, we cannot evaluate their magnitude. It will prove much more useful to look at the mid beam profile of a beam with no slit, and then ask: what would happen now if we make a cut?

Following this line of thought we simulate an ordinary beam under the usual uni-axial compression conditions and recover the buckling branch using the usual protocol. During these simulations we record the vertical stress values for each of the elements in the mid

Version of March 16, 2022– Created March 16, 2022 - 12:40

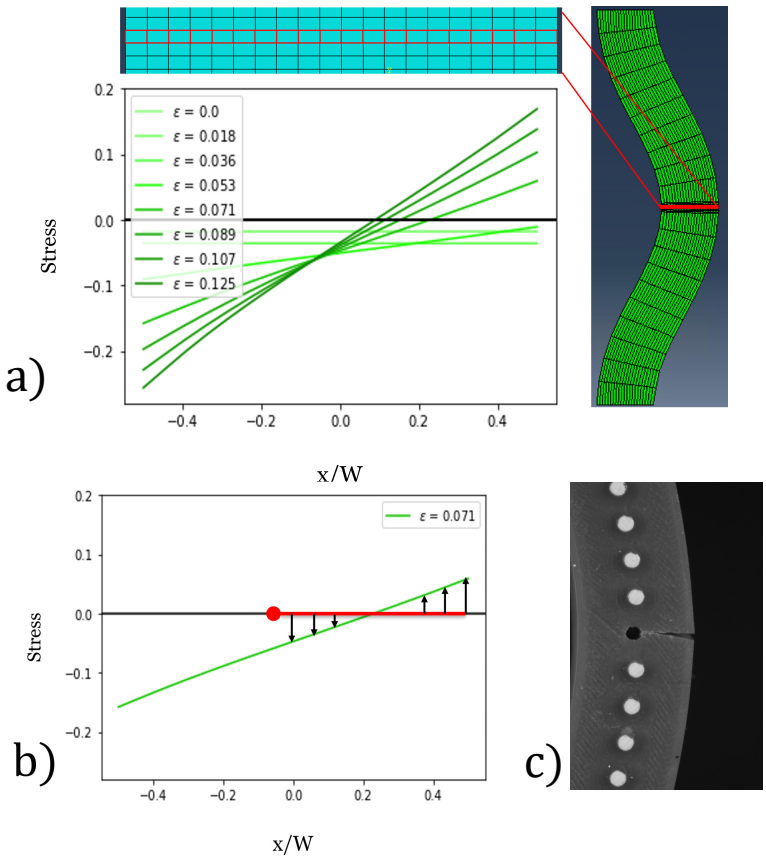

Figure 3.2: *a) Mid beam stress profile of a regular beam for different strains. b) Sketch of the proposed hinge model for the slit opening and the moment exerted into it by the mid beam profile. c) View of a stable configuration of the closed state of a beam with a slit, with the slit partially open.*

beam cross section of the beam, which allows to reconstruct the mid beam stress profile as a function of the applied strain, as shown in figure 3.2 a).

In an ordinary beam, we see that before buckling, the stress profile is constant along the beam, and it increases with the strain (figure 3.2 a). In the post buckling regime, the profile is no longer constant along the mid-beam and becomes monotonically increasing towards the right of the beam with a constant gradient. The profile seems to tilt in a counter clockwise fashion around the middle of the beam, increasing the compressive strains in the left and decreasing them in the right. At the middle of the beam the stresses barely change with the strain.

For big enough ϵ, tensile stresses appear at the right side of the beam, and we define the strain at which the first tensile stresses appear to be ϵ_{ts}. For larger strains than ϵ_{ts} we have now a zone of tensile stresses in the right of the beam, that increases both in extension and magnitude as strains become larger. On the contrary, compressive stresses on the left of the beam become larger with the applied strain. We expect that the appearance of tensile stresses on the right side of the beam to play a role in the opening transition.

We also expect the existence of the slit to be only relevant when tensile stresses are present, as under compression the slit has no effect, and thus ϵ_{ts} is the dividing strain be-

Version of March 16, 2022– Created March 16, 2022 - 12:40

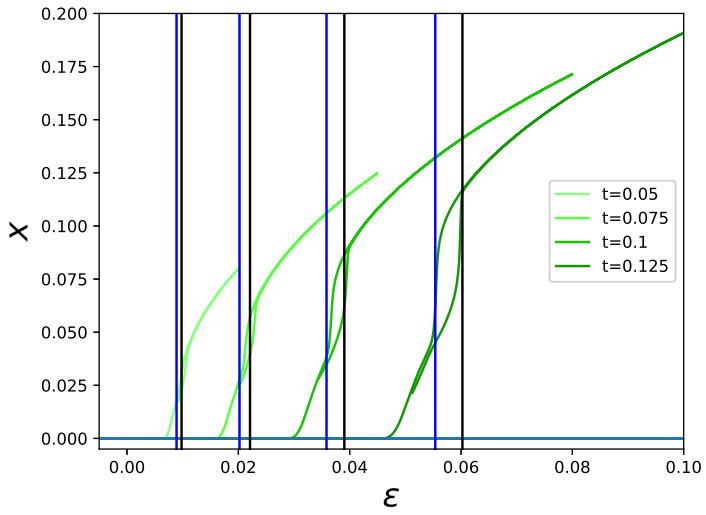

Figure 3.3: *Strain where the first tensile stresses appears ϵ_{ts} (blue) and opening strain ϵ_o prediction using the hinge model (black), over the right branch diagram of beams with a slit with different t.*

tween the two regimes of the closed state. We associate the regime for which the bifurcation diagram of the closed state follows strictly the buckling branch, with the range of strains $\epsilon_b < \epsilon < \epsilon_{ts}$, and expect to see some deviation from the buckling branch in the regime $\epsilon_{ts} < \epsilon < \epsilon_o$. Indeed, in the regime $\epsilon_{ts} < \epsilon < \epsilon_o$ we observe closed stable states where the slit is partially open. In this cases the opening of the slit is smooth, partial and small as seen in figure 3.2 c). In this regime we can observe in the diagram how the state deviates from the ordinary buckling branch, just before the opening transition (figure 3.3).

The equivalence of the left buckled state with ordinary buckling can also be explained by inspecting the mid beam stress profile. When the beam with a slit buckles left, the region with the slit is under highest compressive part of the profile, and it's not exposed to tensile stresses. As so, it behaves like a regular beam for any value of ϵ.

Hinge model for slit opening

We have seen that the slit can partially open without the beam transitioning to the open state, but now we want to find a criteria, based on an analysis of the tensile stresses of the beam, able to predict the strain of the opening transition, ϵ_o.

To asses this problem we think of the slit as a hinge. We consider the top and bottom sides of the slit as rigid surfaces, and the uncut part of the beam as a simple hinge that allows the rigid surface to rotate and open without opposing any resistance (figure 3.2 b). To determine when such a structure will open, we need to look at a change of sign in the total torque applied to the plates of the hinge. Because the beam is symmetric around the mid beam cross section, assessing the change of sign in either the top or bottom plate is enough, as that will happen for the same value of ϵ_o.

Version of March 16, 2022– Created March 16, 2022 - 12:40

We chose the size of the rigid parts to be W/2, regardless of the slit size motivated by two observations. The first observation is that the strain profile rotates around this point, W/2 (figure 3.2 a), and we know that in the profile left of this point, the stresses only get more and more compressive. And the second observation, that we will see in detail later in section 4.1.b, is that the size of the slit has no effect on the opening strain ϵ_o.

We compute the total torque in the slit to predict ϵ_o. In figure 3.3 we show the predicted values with the simulated beam diagrams for four different beams. We find that the prediction are in good agreement with the actual opening event.

It is clear now that the appearance of tensile stresses is critical to understand our system. In the absence of tensile stresses, the slit has no effect, and the behaviour of the beam can be explained by regular buckling. Furthermore, the analysis of the magnitude of these tensile stresses allow us to understand the opening of the slit and opening transition. We can predict the opening strain ϵ_o by understanding that it is triggered by a change of sign in the total moment in the right half of the mid beam. Nonetheless, the importance of tensile stresses is only relevant while the beam is similar to and ordinary beam, that is in the non-buckled, left-buckled and closed state, while we will see in the next section that the behaviour of the beam in the open state is driven by other factors.

3.4 Open state

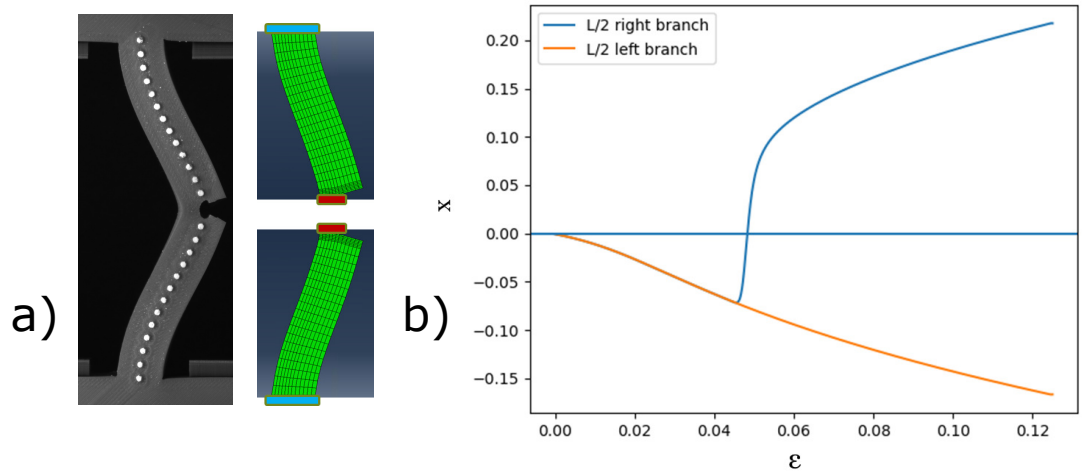

Figure 3.4: *a) Reinterpretation of the beam with a slit as the composition of two half beams with different boundary conditions. The blue rectangle represents boundary conditions fixing the position of both axis, while the red rectangle fixes only the vertical position. b) Bifurcation diagram of the half beam.*

The open state is very different from ordinary buckling and has the distinct characteristic that the top and bottom parts of the slit are never in contact. We want to simulate the open state while always preserving this condition, and we realize that we can do so by only

Version of March 16, 2022– Created March 16, 2022 - 12:40

simulating one half of the beam.

Instead of looking at one single beam with a slit under clamped-clamped boundary conditions we "cut" the beam in half and consider the open state to be a composition of two beams of length L/2, one above the other, as sketched in figure 3.4 a). Each beam has one end clamped, preserving the boundary conditions that we applied to the beam with a slit, and at the "cut" extremes we apply a boundary condition that constrains only it height, allowing for free movement in the horizontal direction. We don't apply any boundary conditions to the top and bottom parts of the slit. We are allowed to make this reinterpretation of the beam by noting that the open state has top-down reflection symmetry. This imposes a boundary condition along the uncut part of the mid beam that restricts its vertical position to be (L-U)/2.

We now simulate only one beam of L/2 under this boundary conditions which allows us to explore the behaviour of the beam in isolation, disregarding any contact that the slit has between its top and bottom parts and allowing us to recover the full bifurcation diagram.

The bifurcation diagram for the half beam shows that when we compress the half beam, starting from an uncompressed straight state, the half beam naturally bends left even for small strains, as seen in figure 3.4 b). The asymmetry of the boundary conditions has broken the symmetry present in regular buckling, and we don't see a regime of null mid beam displacement.

As the half beam naturally bends left, to access the right stable branch of the bifurcation diagram, we compress the beam while applying a lateral load that bends it to the right, that later we turn off progressively to recover the right branch of the diagram during decompression.

When we decompress the beam, the right branch becomes unstable and snaps towards the stable left branch. This phenomenology is similar to the closing event that a beam with a slit undergoes when going from the open state to the closed state (figure 3.5 b).

Now we compare the right branch of the half beam with the right branch of a beam with a slit and find that the branches match well, but it slightly underestimates the closing strain ϵ_c and slightly overestimates the mid beam deflection at large strains, as shown in figure 3.5 b).

We suspect that the small discrepancies between the branches is due to the fact that the boundary condition applied to the "cut" part in the half beam doesn't allow that region to expand, while this is allowed in a beam with a slit. Nonetheless, as the discrepancy is small, we conclude that the half beam is effective in capturing the behaviour of the open state and we trust the full bifurcation diagram obtained as a good representation of the open state in isolation.

Version of March 16, 2022– Created March 16, 2022 - 12:40

Open state as a pre-curved beam

The complete bifurcation diagram of the half beams resembles in its shape the diagram of a pre-curved beam shown in figure 1.2 b). For this reason, we model here a pre-curved beam using the spring model described in section 2.5 and compare it with the half beam.

We obtain the bifurcation diagram of a pre-curved beam using the spring model discussed in methods for different values of k, the ratio between the linear and torsional spring constant, and the natural deflection of the pre-curved beam x_d. By only modifying these two parameters we are able to find a spring system with a bifurcation diagram very similar to the one of the half beams, as seen in figure 3.5 a).

Hence, we can draw a parallelism between the open state of a beam with slit and a pre-curved beam, as the left right symmetry broken by the boundary conditions of the half beam has a very similar effect on the half beam as pre-curving does to an ordinary beam.

The two defining factors of the open state, which are a larger mid beam deflection compared to ordinary buckling and the loss of stability at ϵ_c can be explained by a pre-curved beam. A pre-curved beam reaches further because its longer than an ordinary beam given that the two beams have the same rest length. Also, the pre-curvature of the beam makes the right branch unstable under a critical strain.

3.5 Closing transition

This loss of stability of the right branch of the half beam gives us a clear interpretation of the beam with a slit closing. For $\epsilon < \epsilon_c$ the right branch of a half beam under this boundary conditions is unstable and the system wants to reach the stable left branch. This transition is sharp and hence we observe snapping. In its trajectory the beam with a slit never reaches the stable left branch of the half beam because the top and bottom parts of the slit come into contact, and the beam with a slit changes its state to the closed state.

3.6 Bifurcation Diagram Interpretation

We have enough ingredients now to understand the phenomenology of the right branch of a beam with a slit. The branch is a composition of the bifurcation diagram of a regular beam of length L and a pre-curved beam, joined by the opening event. The opening event, caused by a change of moment in the right half of the beam with a slit, causes the beam with a slit to snap from the buckling curve of a regular beam to the right branch of a half beam bifurcation diagram. Then, when the half beam becomes unstable due to being asymmetric, it snaps again and re-joins the buckling branch of a regular beam, as shown in figure 3.5 b).

We have seen that the asymmetric response of the slit upon compressive or tensile stresses dynamically changes the effective boundary conditions that are imposed on the half beam, allowing the same structure to be in two distinct states and giving the bifurcation diagram

Version of March 16, 2022– Created March 16, 2022 - 12:40

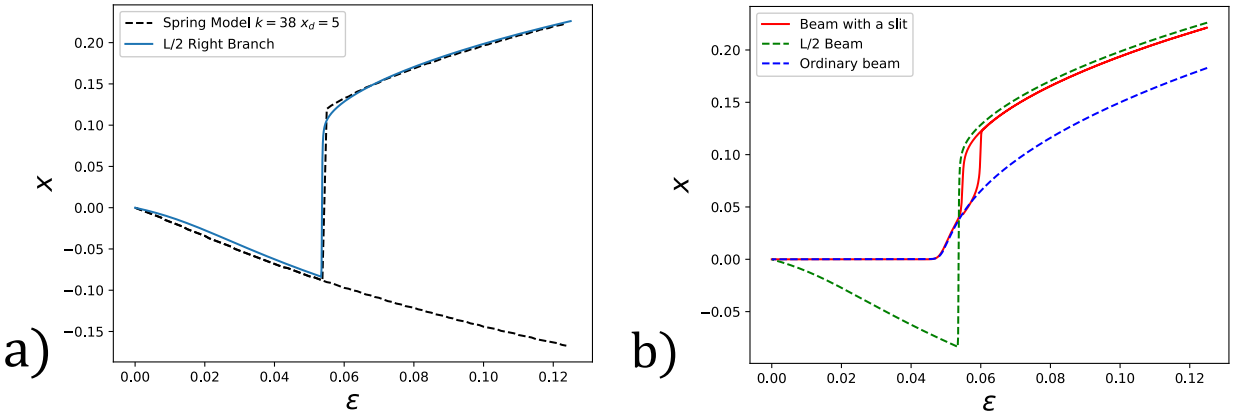

Figure 3.5: *a) Bifurcation diagram obtained for a spring system with $k = 38$ and $x_d = 5$ compared to the bifurcation diagram of a half beam . b) Right branch of the bifurcation diagram of a beam with a slit, together with the right branches of the bifurcation diagrams for an ordinary beam and a half beam.*

of a beam with a slit asymmetry in the post buckling regime as well as an hysteresis loop that creates a strain regime of tristability.

Chapter 4

Beams with slit for metamaterial design

4.1 Role of the beam geometry on the bifurcation diagram

We believe that the beams mechanical response, displayed in the branching diagram in figure 1.4, is ruled by the values of the geometrical dimensionless parameters t = W/L, s = S/W and h = H/W. In this section we will characterize the effect that changing the values of these parameters has on the bifurcation diagram of beams with a slit, with the final goal of being able to predict and tune them during design.

4.1.a Role of the length to width ratio

To assess the effect of t in the diagram of the beam with a slit, we carry on compression experiments and simulations with a set of beams with different t, progressively changing their width W and keeping the height L constant. At the same time, we scale H and S so that the ratios $h = H/W$ and $s = S/W$ are constant trough the beams.

We find that the shape of the bifurcation diagrams of the beams is preserved and displays similar phenomenology, but the diagrams are displaced in the x axis, as seen in figure 4.1 a). To assess if this displacement is the same that we would have in ordinary buckling, we proceed to plot the different diagrams of the beams together in a plot where the horizontal axis is divided by the euler buckling strain and shifted by -1, showing $\frac{\epsilon}{\epsilon_{eb}} - 1$. $\epsilon_{eb} = \frac{t^2\pi^2}{3}$ is the Euler buckling strain for ordinary beams. We can appreciate in figure 4.1 b) that the buckling strain in beams with a slit is proportional to ϵ_b, as we expect knowing that the open state behaves as an ordinary beam.

While the the buckling strain of the different beams is proportional to ϵ_b, we see in figure 4.1 a) that the tristability regimes don't lie on top of each other. This shows that the opening and closing strains ϵ_o, ϵ_c are not strictly proportional to ϵ_b, but there is an extra dependence that shifts the hysteresis regimes to the right for smaller t values.

We collapse the branches so that for all beams $\frac{\epsilon_o}{\epsilon_{eb}} = 0$ and find that the width of the hysteric region, ϵ_o - ϵ_c is proportional to ϵ_b (figure 4.1 c). This means that while we cannot predict the small shifts of the hysteresis regime shown in figure 4.1 b), we know how the

width of the hysteresis regime evolves upon change of the beam's t.

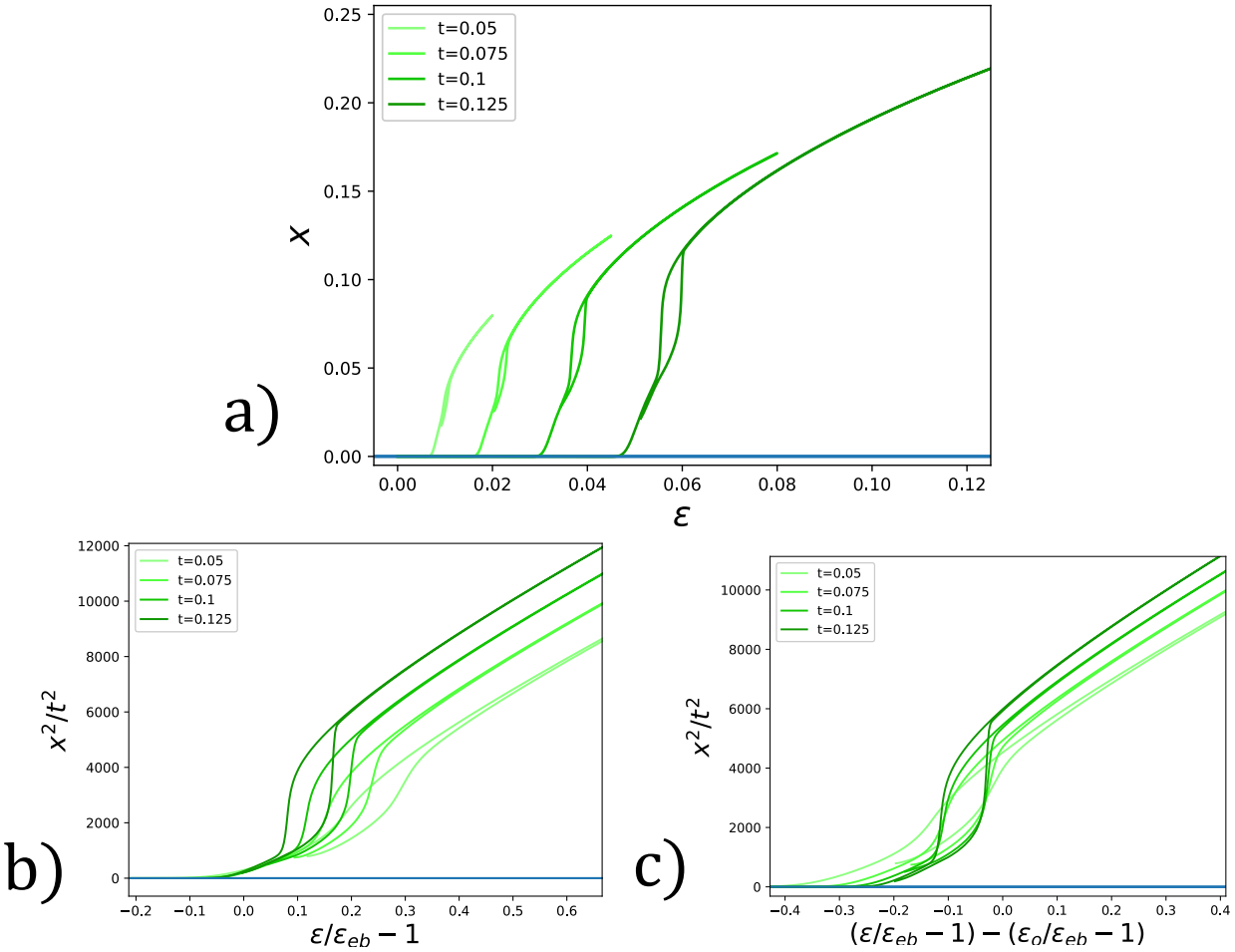

Figure 4.1: *Right buckling bifurcation diagrams for beams with different t, W, and constant L, D, h ($L = 80mm, D = 25mm, t = 0.125, h = 0.25, s = 0.6$). b) The horizontal axis is is re-scaled as $\frac{\epsilon}{\epsilon_b} - 1$ to show that the displacement of the diagrams is similar to ordinary buckling. c) We colapse ϵ_o at 0 to appreciate that all hysteresis loops have the same width.*

4.1.b Role of the slit size

The slit in our beams is the feature that gives beams with a slit new phenomenology when compared to ordinary beams, and thus we expect that changing the size of the slit will have a great effect in a beam with a slit diagram. To explore this dependence, we conduct experiments and simulation in which we systematically modify the slit size s, while keeping all other beam parameters constant.

Figure 4.2 shows the effect of the slit size on the right branch of the bifurcation diagram. We note that the slit size has no effect on the opening strain ϵ_o. All beams open at the same strain, which is surprising. This observation allowed us to realize that the driving factor of the beam opening is the change of moment in the right half of the mid beam, regardless of

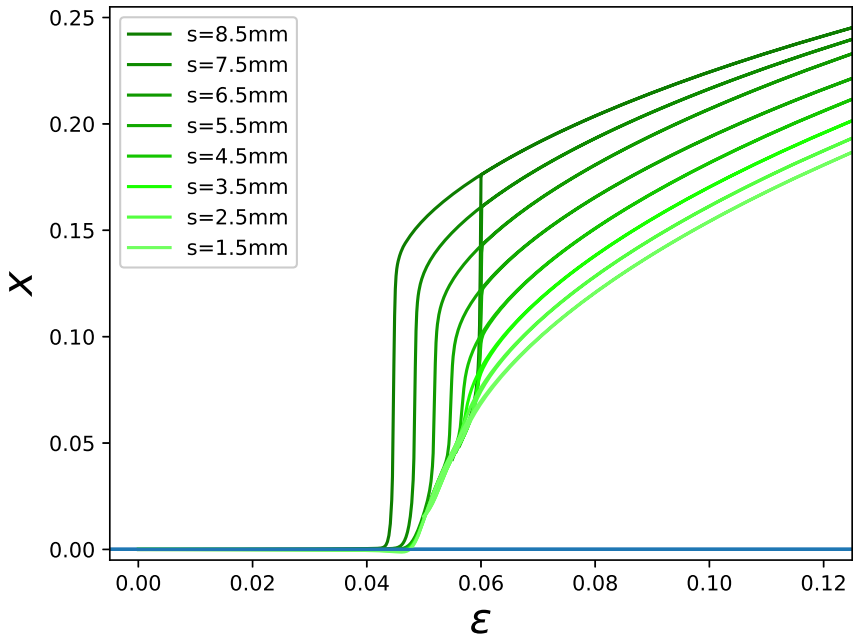

Figure 4.2: *Right buckling bifurcation diagrams for beams with different s and constant L, W, D, h ($L = 80mm, W = 10mm, t = 0.125, D = 25mm, h = 0.2$).*

the slit size, as discussed in section 3.4.

However, we find that the slit size has a significant effect on the mid beam displacement of the open state. While the slit size does not affect the behaviour of the beam while in the closed state, it determines the open state that is reached. Larger s cause a larger mid beam displacement of beams with a slit in the open state.

We also notice that the slit size s has a significant effect in the ϵ_c (figure 4.2). For larger slits, ϵ_c becomes smaller, which makes the tristable regime larger. The closing of the beam is dictated by the open state that is reached, which we have seen that its affected by s.

As we have seen in section 3.5, the size of the slit increases the asymmetry of the beam. In our spring model we understand that as a larger natural deflection, which increases the mid beam deflection of the right branch, in a similar fashion to figure 4.2. The larger slit also implies that the section of the mid beam that is not subject to any boundary conditions is larger, which results in beam with less bending (figure 3.4). In our spring model this is represented with an increase of the ratio k, which has the effect of lowering the minimal stable strain of the right branch. This agrees with the increased stability of the open state seen in figure 4.2.

It's interesting to note that, for slits that are big, of approximately $s > 0.75$, when the beam closes it returns to the non-buckled state, opposite to the usual closing transition to the closed state (figure 4.2). In this regime the symmetry of the beam is recovered after the closing transition, while for smaller slits the symmetry remains broken to the right after clos-

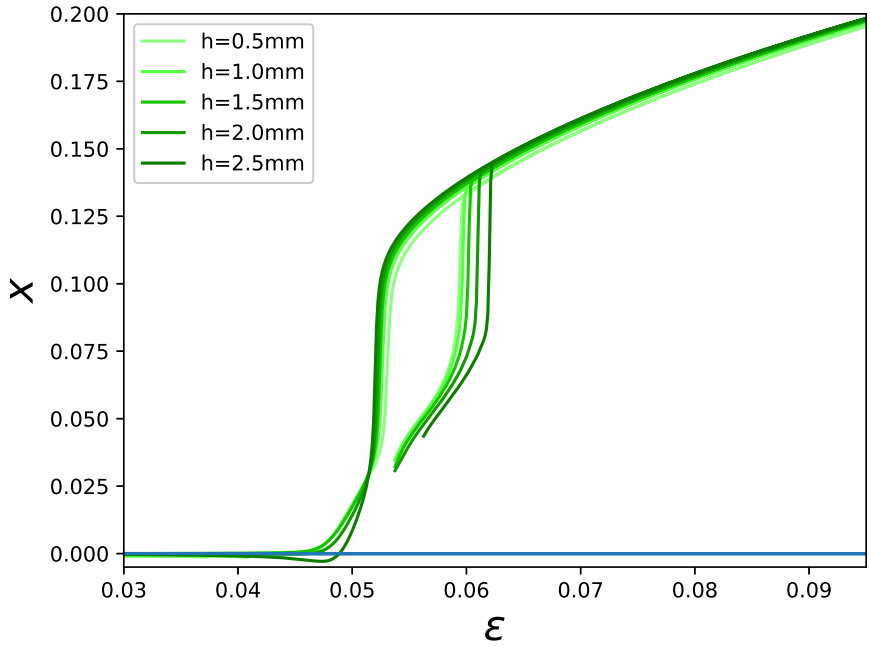

Figure 4.3: *Right buckling bifurcation diagrams for beams with different h and constant L, W, D, s ($L = 80mm, W = 10mm, t = 0.125, D = 25mm, s = 0.6$).*

ing. This recovery of the symmetry might be desired for some matematerial design, and its clear that by only modifying the size of the slit s, we can tune the beam with a slit to have this characteristic.

Small s cause the open state to be closer to the ordinary buckling branch while making the open state less stable. This tendency is consistent with the fact that a beam with slit with s=0 is a an ordinary beam. We observe in 4.2 how smaller s steadily converge to this situation. The snapping transitions get progressively dimmer and the tristability regime becomes smaller as s approaches 0. The behaviour discussed in this work for beams with a slit is clearly present in those with $s > 0.5$, and may be hard to appreciate for lower s values.

4.1.c Role of the hole diameter

We terminate each slit with a small hole, to prevent tearing of the slit. This introduces an additional parameter in the beam. To investigate the effect of the hole we have performed a series of experiments where we systematically vary the hole diameter h (figure 4.3) while keeping the slit s width W and length L of the beam constant.

We focus on the right-buckled branch and find that neither the opening strain ϵ_c nor the mid beam deflection of the open state vary significantly with h (figure 4.3). We interpret this as evidence that the effect of the hole in the open state is very small and can be disregarded during design. In contrast, the opening strain ϵ_o can vary significantly with h shifting to larger strains for increasing h, as shown in (figure 4.3 b).

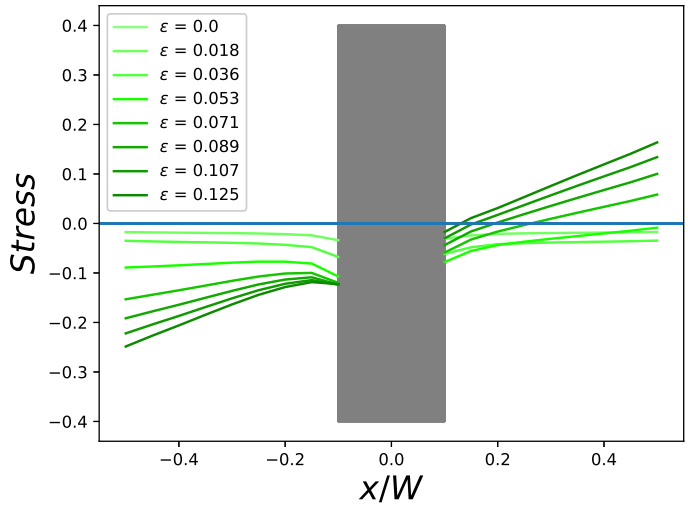

Figure 4.4: *a) Mid beam stress profile of an ordinary beam with a hole of 2mm of diameter in its center, for increasing strains.*

If we recall our arguments in section 3.3 where we argued that the opening is driven by a change of moment on the right half of the mid beam, we can understand why are we seeing ϵ_o increase with h. The presence of the hole perturbs the profile for an ordinary beam shown in figure 3.2, in a way that the change of moment happens at a larger strain.

Figure 4.4 depicts the evolution under compression of the mid beam stress profile in a beam with a centred hole (H = 0.2mm). We see that the profile is similar to the profile of a regular beam without the hole (figure 3.2), the main difference being that stresses around the hole are perturbed and deviate slightly from the typical linear behaviour. Specifically, we see the stresses to be more compressive around the hole than what they would be if they followed the linear trend of the profile. We understand that this is an effect of the hole acting as an arch and translating the stresses towards the support points in the sides.

For small h, $h < 0.15$, the snap out compression will be well approximated by the linear profile as the ϵ_o increase with h is slow. As h gets larger the increase with h is faster and the effect more noticeable. This allows us to not worryabout the hole effet for small h, while we can use it to tune the tristability regime using large h values in our design.

Role of the length L

We expect beams with a slit to display equivalent mechanical responses in a wide range of scales, which facilitates the incorporation of beams with a slit in the design of different sized metamaterials. To check if this holds, we manufacture beams of different lengths L and scale all three other relevant beam parameters, s, h, and t so that the proportions are preserved and we carry out compression experiments. As simulations are dimensionless, they are inherently scale free and we only do this experimentally. We find that the scaled bifurcation

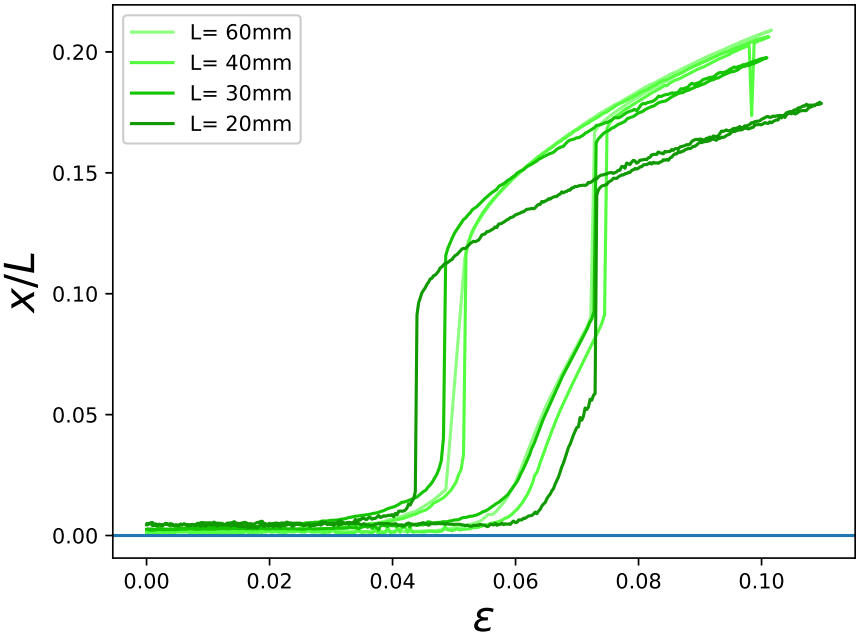

Figure 4.5: *Right buckling bifurcation diagrams for beams with different L and proportionally scaled t=0.125, s = 0.6 ,h = 0.25*

diagrams are roughly equivalent (figure 4.5), confirming that we can confidently scale our results to fit manufacturing requirements.

4.2 Simulations vs Experiments

We have carried out the above analysis using data from FEM simulations. Now we will compare the bifurcation diagrams from FEM simulations to our experimental data, as we ultimately we are interested in designing real meta-materials.

We find that the phenomenology described in this chapter is still true for real beams, as seen in figure 4.6. Beams with different t are displaced following a t^2 scaling, and the width of the hysteretic regime also scales as t^2. For beams with different slit sizes we again see that the opening strain ϵ_o is constant, while the hysteretic regime grows with the slit size. Finally beams with different hole sizes show a monotonic increase of ϵ_o, with the hole diameter, while keeping the closing strain ϵ_o constant. Notably, not only this tendencies hold for real beams, but direct comparison of of the diagrams also holds well. The compression branch is very similar, while the decompression branch deviates slightly from what is seen in the simulations due to creep (figure 4.6).

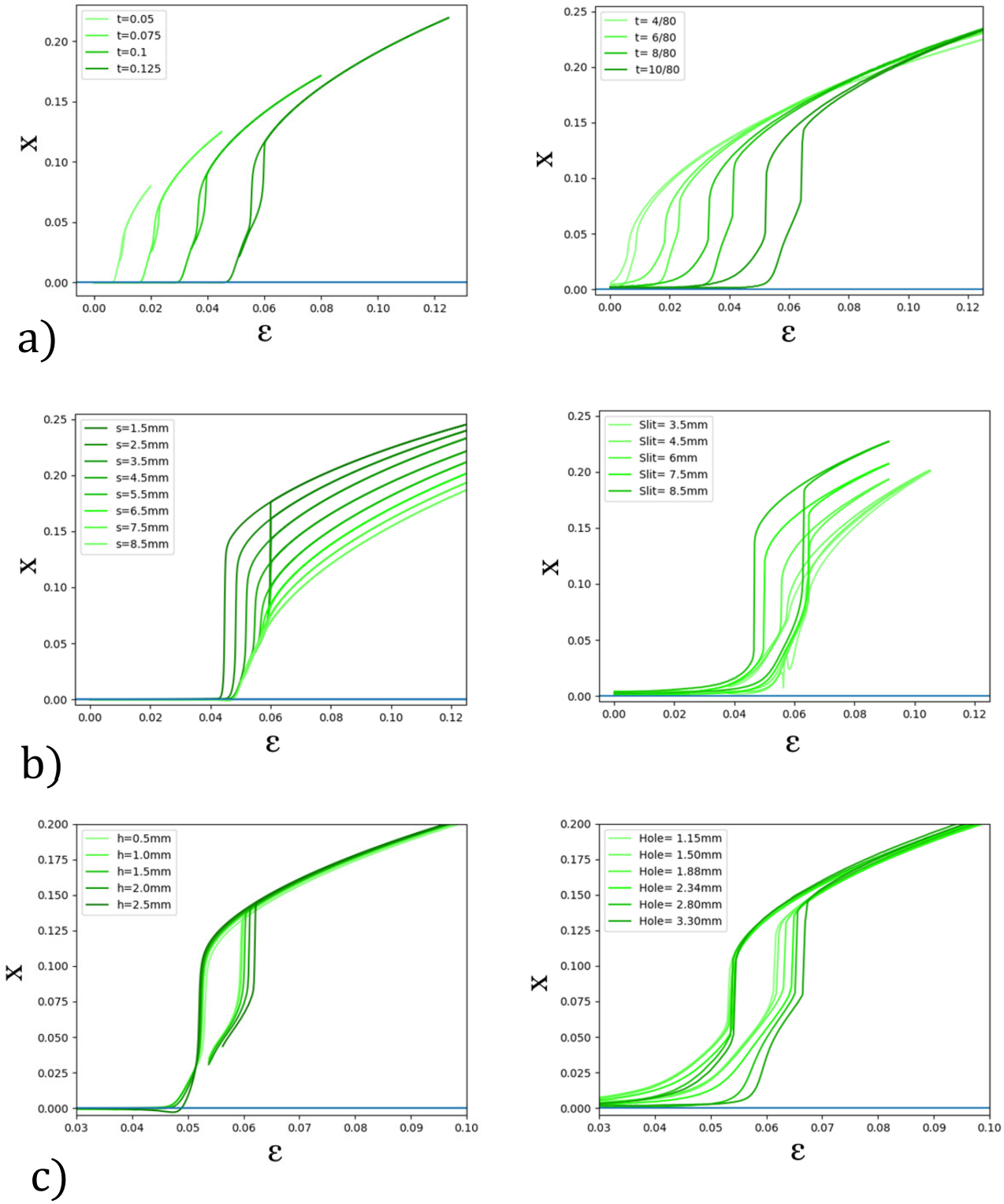

Figure 4.6: *Comparation of the bifurcation diagrams obtained using Abaqus/CAE simulations with the bifurcation diagrams obtained doing uniaxial compression experiments.*

4.3 Using beams with a slit in metamaterials

We will see in this section how we can use the particular shape of the bifurcation diagram of a beam with slit, seen in the previous sections, to achieve functionality in metamaterials, and we will see that there are mainly two distinct properties of the beams that are interesting.

The first property, is that we can use the fact that the diagram is symmetric in the pre-buckling and initial post-buckling regime to decide the buckling direction with only a small perturbation, and then propagate and amplify it using the asymmetric response in the post buckling regime. In the counting beams that inspired this work [4], the small perturbation is in the form of contact with a thinner neighbouring beam. This contact decides the buckling direction. Later, the if the beam is in the right branch, it will snap and enter in contact with a neighbouring thinner beam, changing its buckling direction. On the contrary, if the beam buckles left, it does not reach far enough to enter in contact with a neighbouring beam and the "signal" does not propagate.

We can also use beams with a slit as hysterons under compression due to the existence of a hysteresis loop in the right branch diagram. Hysterons are relevant in metamaterials because they can encode memory effects [6]. Using beams with a slit as hysterons has two distinct properties that might be of interest. The first is that the field applied to make the beam snap (compression) is perpendicular to the direction of snapping. The second property is that, as we have seen, beams with a slit are tristable in the hysteresis loop and have one extra stable state, opposed to the usual bistability of hysterons. Figure 4.7 shows two independent beams with a slit that together make a system that has a particular transition graph, determined by the specific hysteresis regimes of both beams. In this case the hysteresis regime of the left beam is inside the hysteresis regime of the right beam. We can note that in this simple system we already have some sense of memory. To reach state 01 we need to have compressed and then decompressed the system, giving us some information of past events.

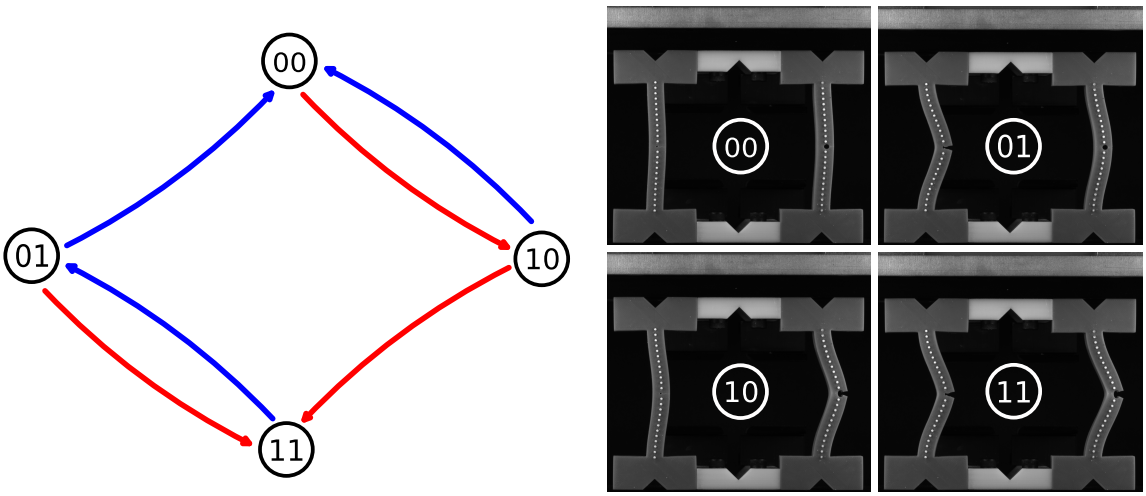

Figure 4.7: *Example of the use of beams with slit as hysterons. We define the closed state as 0 and the open state as 1. This particular diagram result from the system of two independent hysterons with one hysteresis loop (left beam) inside the other beam hysteresis loop (right beam).*

Chapter 5

Conclusion and discussion

We conclude that beams with a slit provide a new beam design that can be used in metamaterials to obtain a tuneable asymmetric response in the post-buckling regime after symmetric buckling. Additionally, we have found that the open and closed states of beams with a slit present hysteresis upon compression and decompression with snappy transitions between the states, which opens the possibility of using beams with a slit as mechanical hysterons [6].

We understand now the bifurcation diagram of beams with a slit. The bifurcation diagram combines the bifurcation diagrams of an ordinary beam and a pre-curved beam, united by a snapping transition. The beam with a slit behaves like an ordinary beam while the stresses in the mid beam are compressive everywhere, a regime in which the slit has no effect. In the open state, we have seen that its behaviour can be captured by a half beam whose bifurcation diagram is shaped as that of a pre-curved beam, due to the asymmetry of its boundary conditions. The beam with a slit can transition from the closed to the open state due to a change of moment in the right half of the mid beam, that opens the beam, uniting the two diagrams.

We have also seen how we can tune the mechanical response of beam with a slit by modifying its geometrical parameters. The size of the slit controls the degree of asymmetry in the post buckling regime, increasing its mid beam deflection and making the open state more stable, which increases the tristability strain regime of the beam. The size of the hole can be used to increase the same tristability regime without making the open state more stable. It's also possible to modify the buckling strain of the beam by changing its (width to length ratio) t.

As of now, we know of one structure that uses beams with a slit to achieve its functionality, the counting beams [4]. This structure uses the asymmetrical response of the post buckling regime to propagate a signal in only one direction. The ability of beams with a slit to buckle left or right depending on small perturbations, for example a small lateral force due to contact, and having a much stronger post-buckling response than this perturbation upon snapping and opening makes them a good amplifier of such perturbations.

As a hysteron, beams with a slit have two unusual properties. Beams with a slit are hysterons under a force perpendicular to its snapping direction and are tristable, opposed to

the usual bistability of other hysterons, introducing an extra state that may prove useful in finding unusual transition graphs.

Bibliography

[1] X. Ren, R. Das, P. Tran, T. D. Ngo, and Y. M. Xie, *Auxetic metamaterials and structures: A review*, 2018.

[2] T. Bückmann, M. Thiel, M. Kadic, R. Schittny, and M. Wegener, *An elasto-mechanical unfeelability cloak made of pentamode metamaterials*, Nature Communications **5** (2014).

[3] L. Kwakernaak, *Designing Counting Metamaterials*, 2020, [Master Thesis]. Leiden University student repository. https://hdl.handle.net/1887/94288.

[4] L. Kwakernaak and M. V. Hecke, *Counting Beams*, [Manuscript in preparation], 2022.

[5] L. Lubbers, *Mechanical metamaterials: nonlinear beams and excess zero modes*, 2018, [Doctoral Thesis]. Leiden University student repository. https://hdl.handle.net/1887/65383.

[6] H. Bense and M. V. Hecke, *Complex pathways and memory in compressed corrugated sheets*, PNAS **Vol. 118** (2021).